

## A Model for the Activated Energy Transfer within Eumelanin Aggregates

Susan E. Forest,<sup>†,‡</sup> Wai C. Lam,<sup>§</sup> David P. Millar,<sup>§</sup> J. Brian Nofsinger,<sup>†</sup> and John D. Simon<sup>\*,†,||</sup>

Department of Chemistry, Duke University, Durham, North Carolina 27708, Department of Molecular Biology, The Scripps Research Institute, La Jolla, California 92037, and Department of Biochemistry, Duke University, Durham, North Carolina 27708

Received: June 25, 1999; In Final Form: October 1, 1999

The emission properties of eumelanin from *Sepia officinalis* are examined following UV-A excitation. The emission decay is nonexponential, exhibiting decay components on the tens of picosecond to several nanosecond time scales. The corresponding depolarization dynamics are also nonexponential and reveal that the emission becomes totally depolarized with an average time constant of  $\sim 80$  ps at 20 °C. The depolarization of the emission is found to be activated; a simple Arrhenius fit to the depolarization rate data gives an activation barrier of  $21 \pm 3$  kJ mol<sup>-1</sup>. The nonexponential emission decay is concluded to be a reflection of the structural disorder of eumelanin. The rapid and nonexponential depolarization dynamics are attributed to energy transfer processes that occur within “spherical” subunits that comprise the eumelanin aggregates.

A dominant cause of skin damage and skin cancer is exposure to ultraviolet (UV) radiation. While significant attention has been paid to UV-B (280–320 nm) exposure<sup>1,2</sup> (the region of direct DNA absorption), it is becoming clear that UV-A (320–400 nm) radiation also plays an important role in skin diseases.<sup>1,3,4,5</sup> A major UV-A photoreceptor in melanocytes, the cells that give rise to melanoma, is melanin. Therefore, elucidating the photophysical and photochemical properties of melanin is important for understanding the biological role(s) played by this pigment. There are two main types of melanin. Eumelanins are brown to black pigments formed from the oxidation of dopa, while pheomelanins are yellow to red pigments formed from the oxidation of dopa in the presence of cysteine. In this study we focus on eumelanin isolated from *Sepia officinalis*, which is considered to be a model system for the human pigment.<sup>6</sup>

For melanin to act as a photoprotecting agent, which is believed to be one of its more important functions,<sup>7</sup> the pigment must be able to dissipate absorbed light energy without undergoing any adverse photochemical reactions. Using photoacoustic spectroscopy, we have shown that eumelanin dissipates UV-A radiation on the subnanosecond time scale with nearly unit quantum efficiency.<sup>8</sup> However, some photochemistry does occur in this wavelength range. Specifically, excitation of eumelanin by UV-A light produces reactive oxygen species.<sup>9,10</sup> This difference in photochemistry may in part be attributed to the varying size of eumelanin particles.<sup>11</sup> In this communication, emission spectroscopy and scanning electron microscopy are utilized to gain insight into the photophysical processes that occur in large eumelanin aggregates following the absorption of UV-A radiation.

Eumelanin from *S. officinalis* was purchased from Sigma. A 40 mg sample of eumelanin was solubilized in 40 mL of potassium phosphate buffer, pH 7.2. The solution was sonicated for 30 min and then centrifuged for 30 min. The aqueous

solution was filtered with a 0.2  $\mu$ m filter to further remove unsolubilized particles. For collection of the emission spectrum, the sample was excited by the tunable output of a regeneratively amplified Ti:sapphire/OPA laser system (Spectra Physics). The emission was focused into a Spex 270 M monochromator (Instruments S.A., Inc) by two paraboloidal off-axis mirrors (Janos Technology, Inc.), and the spectrum was recorded by a liquid nitrogen-cooled, front-illuminated, UV-enhanced CCD (Instruments S.A., Inc). The time-dependent emission was measured using time-correlated single photon counting.<sup>12</sup> Briefly, samples contained in quartz cuvettes (1 cm path length) were excited at 335 and 310 nm using the frequency-doubled output from a synchronously mode-locked and cavity-dumped dye laser (Coherent 702). Sample emission was collected at right angles to the excitation beam, collimated by a lens, passed through a motor-controlled polarizer, and focused on the entrance slit of a monochromator (JY H-10). Emission at 420, 508, and 520 nm was examined. To measure population decay, the analyzing polarizer was set to the magic angle, 54.7°, with respect to the polarization of the excitation beam. For anisotropy decay measurements, the emission polarizer was alternated between vertical and horizontal directions every 30 s and the decays collected with each polarizer setting were accumulated in separate memory segments of the multichannel analyzer. Anisotropy and lifetime measurements were performed at 10, 20, and 30 °C.

Figure 1 shows the steady-state emission spectrum of the eumelanin sample using an excitation wavelength of 335 nm. Figure 2 shows the corresponding population decay recorded at 420 nm and 20 °C. To obtain an acceptable  $\chi^2$  value, a sum of four exponential functions is required. The resulting time constants and amplitudes for such a functional fit to the data are given in Table 1 for the three emission wavelengths studied. The data in Table 1 show that the dynamics are essentially independent of the emission wavelength probed. Emission dynamics at 420 and 508 nm were also recorded using an excitation wavelength of 310 nm (data not shown). These data are essentially the same as that observed for 335 nm excitation. It is interesting to note that related studies on bovine and human

\* To whom correspondences should be sent.

<sup>†</sup> Department of Chemistry, Duke University.

<sup>‡</sup> Current address: The Procter and Gamble Co., Miami Valley Labs, 11810 East Miami River Rd, Ross, OH 45061.

<sup>§</sup> The Scripps Research Institute.

<sup>||</sup> Department of Biochemistry, Duke University.

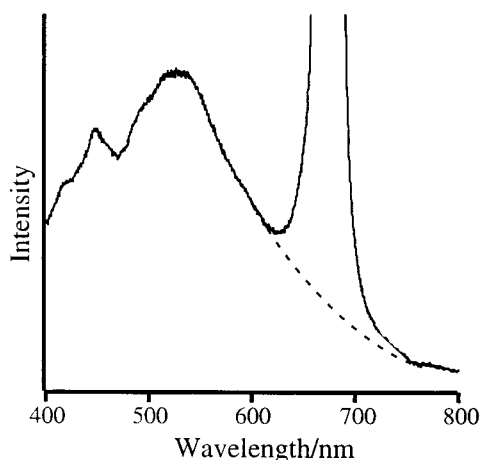


**Figure 1.** Uncorrected emission spectrum of *Sepia* eumelanin upon excitation at 335 nm. The emission quantum yield is  $\leq 10^{-2}$ . The peak at 670 nm is the second-order diffraction of the excitation light. The dashed line indicates the shape of the emission spectrum in this region as revealed by using a 266 nm excitation wavelength.

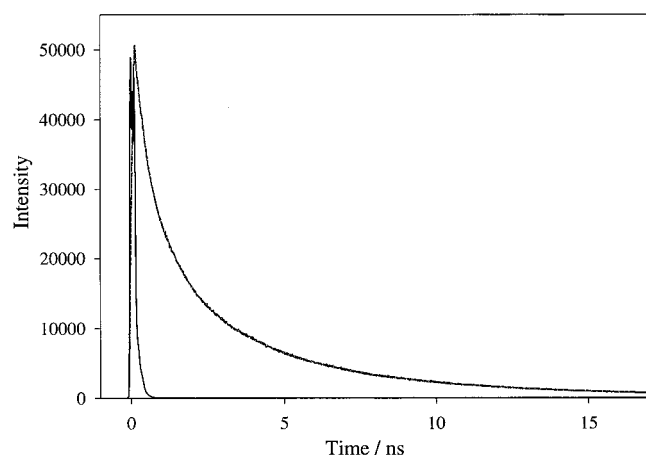


**Figure 2.** Time-dependent emission dynamics of eumelanin at 420 nm following excitation at 335 nm. The instrument response function is also shown. A calculated decay using a convolution of the instrument response function, and a sum of exponentials using the parameters given in Table 1 is superimposed on the experimental data.

**TABLE 1: Fitting Parameters for the Magic Angle Emission Decays at 420, 508, and 520 nm for Eumelanin at 20 °C Following Excitation at 335 nm<sup>a</sup>**

	420 nm	508 nm	520 nm
$\tau_1$ ( $\alpha_1$ )	59 (0.51)	62 (0.52)	58 (0.54)
$\tau_2$ ( $\alpha_2$ )	525 (0.21)	557 (0.23)	505 (0.22)
$\tau_3$ ( $\alpha_3$ )	2141 (0.19)	2082 (0.16)	2965 (0.16)
$\tau_4$ ( $\alpha_4$ )	6429 (0.09)	7204 (0.08)	7054 (0.08)
$\chi^2$	1.19	1.14	1.17

<sup>a</sup> Time constants,  $\tau_i$ , are in picoseconds;  $\alpha_i$  are the corresponding amplitudes.

(from the retinal pigment epithelium) eye melanins also found that the fluorescence decay is fit best using four exponentials.<sup>13</sup> The values obtained in that study are similar to those reported in Table 1, which is consistent with the belief that *Sepia* eumelanin is a good model for human eumelanin. They also reported that the emission dynamics do not vary significantly as a function of the wavelength studied, in agreement with our data.

We now turn to a discussion of the emission anisotropy measurements ( $\lambda_{\text{ex}} = 335$  nm,  $\lambda_{\text{pr}} = 420$  nm) recorded at 10, 20, and 30 °C. The emission anisotropy is defined by<sup>14</sup>

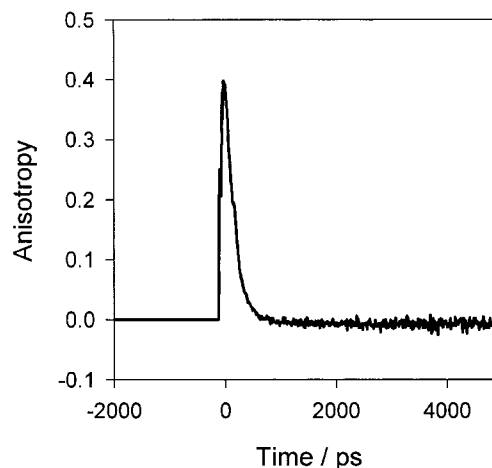


**Figure 3.** Time-dependent anisotropy for the emission of eumelanin at 420 nm following excitation at 335 nm at 20 °C. The initial anisotropy is 0.35, and a fit of the data to a single exponential gives a decay of time of 83 ps ( $\chi^2 = 1.32$ ).

**TABLE 2: Temperature-Dependent Anisotropy Parameters for Eumelanin Emission at 420 nm Following Excitation at 335 nm**

	$T = 10$ °C	$T = 20$ °C	$T = 30$ °C
$r_0$	0.34	0.35	0.36
$\tau/\text{ps}$	114	83	67
$\chi^2$	1.26	1.32	1.23

$$r(t) = I_{\parallel}(t) - I_{\perp}(t)/I_{\parallel}(t) + 2I_{\perp}(t) \quad (1)$$

where  $I_{\parallel}$  and  $I_{\perp}$  are the emission intensities parallel and perpendicular to the polarization of the excitation beam, respectively. The function  $r(t)$  was fit to a single-exponential function,  $r(t) = r_0 \exp(-t/\tau)$ , where  $r_0$  is a constant and  $\tau$  is the depolarization time. The results are presented in Table 2 and Figure 3. If the absorption and emission transition dipoles are parallel to one another, then  $r_0 = 0.4$ .<sup>14</sup> The values for  $r_0$  listed in Table 2 are close to this theoretical value. The data in Table 2 show that the depolarization time decreases with increasing temperature. Therefore, the dynamics that occur following excitation must be activated. An Arrhenius fit to the temperature-dependent data gives an activation energy of  $21 \pm 3$  kJ mol<sup>-1</sup>. It is important to note that the  $\chi^2$  values obtained for the single exponential fit to  $r(t)$  are generally poor, which suggests that like the population dynamics, the depolarization dynamics are also more complicated than a simple exponential function.

In general, the dynamics of the depolarization of emission are attributed to the rotational motion of the excited molecule. However, this is not likely the mechanism in the case of eumelanin. Detailed studies of the structure of eumelanin using scanning electron microscopy (SEM) reveal that *Sepia* eumelanin is composed of nearly spherical subunits varying in size that cluster into irregularly shaped aggregates ranging in size from 2 to 25  $\mu\text{m}$  in diameter.<sup>15–18</sup> Figure 4 presents a scanning electron micrograph of such a typical eumelanin aggregate.<sup>18</sup> For a diameter of 2  $\mu\text{m}$ , the Stokes–Einstein–Debye (SED) equation<sup>19</sup> predicts a rotational time of 0.76 s, which is 11 orders of magnitude longer than the depolarization dynamics observed. Because this is unreasonable, we could propose that the excitation energy is localized on one of the subunits that comprise a melanin aggregate, and emission depolarization occurs through rotation of that particle within the pigment aggregate. While it is difficult to estimate the effective viscosity of this environment, for discussion purposes, we will take the

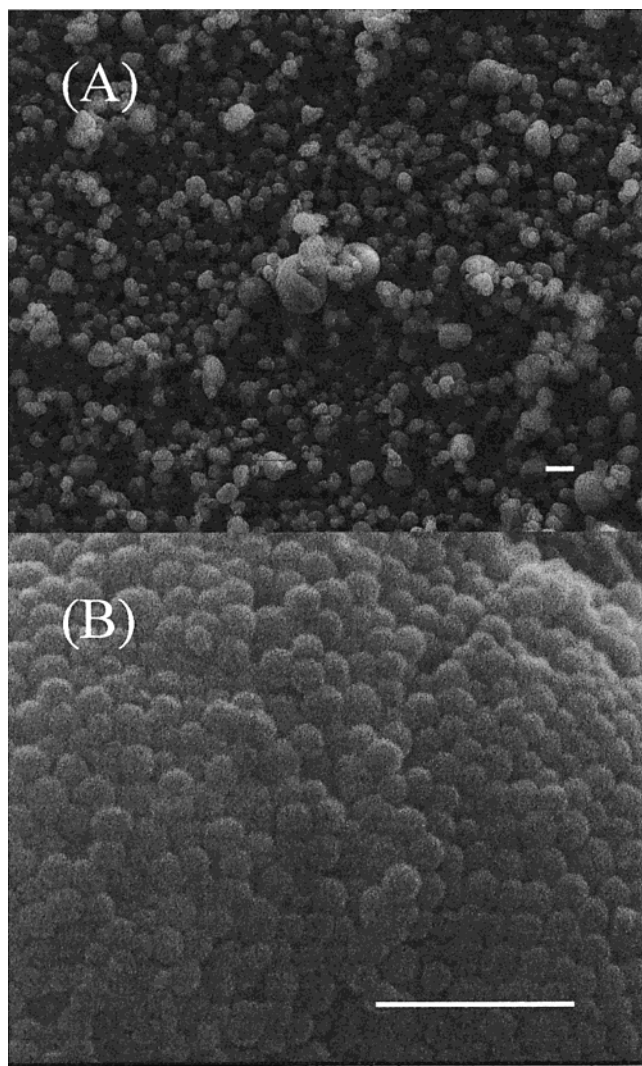


**Figure 4.** Scanning electron micrographs of *Sepia* melanin: (A) dry sample of *Sepia* melanin (reference bar = 142.8  $\mu\text{m}$ ); (B) enlargement of one of the particles in (A) (reference bar = 0.714  $\mu\text{m}$ ). (B) shows that the large melanin particles (2–25  $\mu\text{m}$  in diameter) in (A) are composed of smaller subunits that range from 50 to 250 nm in diameter.<sup>18</sup>

viscosity to be that of the water solvent. This then predicts a rotation time for a 70 nm particle (the small end of the particle distribution) to be  $3.3 \times 10^{-5}$  s, which is still an unreasonable 6 orders of magnitude slower than the depolarization time observed. If we use the SED expression and calculate the radius that would correspond to an observed rotation time of  $\sim 80$  ps, we obtain  $r = 950$  pm, which is unrealistically small given the reported particle-size distributions for eumelanin.<sup>15–18</sup> It is also clear that the calculated and experimental times cannot be brought into agreement by the standard corrections applied to the SED theory.<sup>20</sup> Therefore, it is simply not reasonable to assign the observed behavior to rotational dynamics of the eumelanin aggregates.

We attribute the rapid depolarization of the emission to energy transfer processes between chromophores that comprise eumelanin. The emission data reveal that the transfer of energy occurs rapidly and results in complete depolarization of the emission. Such behavior requires that the number of donor and acceptor sites present in a melanin subunit be sufficient so that the transition dipoles of the embedded “molecular emitters” cover all possible orientations in three dimensions. Because of the complexities of eumelanins, specific details of the chemical

structure of the pigments have not been determined. Thus, the identity of the molecular chromophores that are involved in the energy transfer process remains unknown. Some insight can be gained, however, from the studies of eumelanins using X-ray scattering techniques and molecular microscopies. Small-angle X-ray scattering studies suggest that the molecular unit is rodlike in shape, 4.8–8.5 nm long and 0.6–0.8 nm in diameter.<sup>21–23</sup> Qualitatively similar models have been proposed for melanins including *Sepia* melanin on the basis of ultrasonic measurements.<sup>24–26</sup> Using wide-angle X-ray diffraction of dried melanin samples and STM of monolayers of the melanin polymer on graphite, the fundamental building block of the polymer of synthetic melanin was proposed to be a three-sheet stacking structure that has a lateral dimension of 2.0 nm and a height of 0.76 nm and consists of 15–24 5,6-indolequinone residues.<sup>27</sup> A modeling of X-ray diffraction data of several melanins (including *Sepia*) by Cheng et al. gives a slightly different dimension of a fundamental melanin unit, which is hypothesized to contain a four-layer stacking of 4–8 5,6-dihydroxyindole or 5,6-indolequinone units per layer.<sup>28,29</sup>

If we take the average diameter of a melanin subunit to be 150 nm (the peak of the particle size distribution),<sup>15–17</sup> and consider these substituted indolequinone residues to be the chromophores within melanin, then the molecular structure model of Cheng et al.<sup>28,29</sup> suggests that there are tens of millions of such chromophores within the subunit structure. If energy transfer occurs between these chromophores, a small fraction of this number is sufficient for complete depolarization of the emission by energy transfer. It is important to realize that these chromophores are likely to be in different local environments because of the molecular heterogeneity of the polymer. Therefore this collection of chromophores will exhibit a distribution of excited electronic state energies. The fact that the initial anisotropy is close to the theoretical maximum of 0.4 indicates that initial emission transition dipole is nearly parallel to the absorption transition dipole. Energy transfer can then occur to acceptors that are situated in close proximity to the initial absorber giving rise to the observed emission depolarization on the picosecond time scale. Energy transfer generally occurs to an acceptor site that has an electronic energy less than or equal to that of the donor. But, because of the structural heterogeneity of the polymer (on both the microscopic and macroscopic distance scales) and the large number of chromophores within the structure, some of the surrounding chromophore that could be considered as “acceptor sites” will have excited state energies that are slightly higher in energy than that of the donor. Energy transfer to an acceptor that has an energy slightly greater than that of the donor can occur, if the energy difference is on the order of the thermal energy available to the system. The efficiency and rate of such energy transfer processes increase with increasing temperature because more acceptor sites become accessible with the increased thermal energy.<sup>30</sup> Such a model would be characterized by an activated energy transfer, which is consistent with the trend of the temperature-dependent depolarization times reported in Table 2. We are currently examining the emission dynamics from single melanin particles in order to assess the validity of this model. The results from those experiments will be reported at a later date.

**Acknowledgment.** This work is supported by the National Institute of General Medical Sciences. We thank Leslie Eibest for her contributions to this work.

## References and Notes

- (1) Kvam, E.; Tyrrell, R. M. *Carcinogenesis* **1997**, *18*, 2379–2383.



- (2) Madronich, S.; DeGrujil, F. R. *Photochem. Photobiol.* **1994**, 59, 541–546.
- (3) Peak, M. J.; Peak, J. G.; Churchill, M. E. In *Biological responses to Ultraviolet A Radiation*; Urbach, F., Ed.; Valdenmar Publishing: KS, 1992; pp 39–45.
- (4) Ranadive, N. S.; Menon, I. A. *Pathol. Immunopathol. Res.* **1986**, 5, 118–139.
- (5) Williams, R. J. P. In *The Biology and Chemistry of Active Oxygen*; Bannister, J. V., Bannister, W. H., Eds.; Elsevier: New York, 1984; pp 1–15.
- (6) Kollias, N.; Sayre, R. M.; Zeise, L.; Chedekel, M. R. *J. Photochem. Photobiol. B: Biol.* **1991**, 9, 135.
- (7) Hill, H. Z. *BioEssays* **1992**, 14, 49.
- (8) Forest, S. E.; Simon, J. D. *Photochem. Photobiol.* **1998**, 68, 296.
- (9) Felix, C. C.; Hyde, J. S.; Sarna, T.; Sealy, R. C. *Biochem. Biophys. Res. Commun.* **1978**, 84, 335.
- (10) (a) Sarna, T. *J. Photochem. Photobiol. B: Biol.* **12**, 215. (b) Reszka, J.; Jimbow, K. In *Oxidative Stress in Dermatology*; Fuchs, J., Packer, L., Eds.; Marcel Dekker: New York, 1993; pp 287–320.
- (11) Nofsinger, J. B.; Forest, S. E.; Simon, J. D. *J. Phys. Chem.*, submitted for publications
- (12) Guest, C. R.; Hochstrasser, R. A.; Dupuy, C.; Allen, D. J.; Benkovic, S. J.; Millar, D. P. *Biochemistry* **1991**, 30, 8759.
- (13) Docchio, F.; Boulton, M.; Cubeddu, R.; Ramponi, R.; Barker, P. D. *Photochem. Photobiol.* **1991**, 54, 247–253.
- (14) Lakowicz, J. R. *Principles of Fluorescence Spectroscopy*; Plenum Press: New York, 1983.
- (15) Zeise, L.; Addison, R. B.; Chedekel, M. R. *Pig. Cell Res. Suppl.* **1992**, 2, 48.
- (16) Zeise, L.; Murr, B. L.; Chedekel, M. R. *Pig. Cell Res.* **1992**, 5, 132.
- (17) Chedekel, M. R.; Ahene, A. B.; Zeise, L. *Pig. Cell Res.* **1992**, 5, 240.
- (18) Nofsinger, J. B.; Forest, S. E.; Eibest, L.; Gold, K. A.; Simon, J. D. *Pigm. Cell Res.*, submitted.
- (19) Tau, T. *Biopolymers* **1969**, 8, 609.
- (20) Simon, J. D.; Thompson, P. A. *J. Chem. Phys.* **1990**, 92, 2891 and references therein.
- (21) Miyake, Y.; Izumi, Y. In *Structure and Function of Melanin*; Jimbow, K., Ed.; Sapporo: Fujishoin, 1984; Vol. 1, pp 3–13.
- (22) Miyake, Y.; Izumi, Y.; Yasuda, K.; Jimbow, K. In *Structure and Function of Melanin*; Jimbow, K., Ed.; Sapporo: Fujishoin, 1985; Vol. 2, pp 3–10.
- (23) Miyake, Y.; Izumi, Y.; Tsutsumi, A.; Jimbow, K. In *Structure and Function of Melanin*; Jimbow, K., Ed.; Sapporo: Fujishoin, 1987; Vol. 4, pp 32–43.
- (24) Kono, R. In *Structure and Function of Melanin*; Jimbow, K., Ed.; Sapporo: Fujishoin, 1984; Vol. 1, pp 14–17.
- (25) Kono, R.; Jimbow, K. In *Structure and Function of Melanin*; Jimbow, K., Ed.; Sapporo: Fujishoin, 1985; Vol. 2, pp 11–18.
- (26) Kono, R.; Yoshizaki, H. In *Structure and Function of Melanin*; Jimbow, K., Ed.; Sapporo: Fujishoin, 1987; Vol. 4, pp 24–31.
- (27) Zajac, Z. W.; Gallas, J. M.; Cheng, J.; Eisner, M.; Moss, S. C.; Alvarado-Swaigood, A. E. *Biochim. Biophys. Acta* **1994**, 1199, 271.
- (28) Cheng, J.; Moss, S. C.; Eisner, M.; Zschack, P. *Cell Res.* **1994**, 7, 255.
- (29) Cheng, J.; Moss, S. C.; Eisner, M. *Pig. Cell Res.* **1994**, 7, 263.
- (30) Parichha, T. K.; Acharyya, T. K.; Ray, R. D.; Talapatra, G. B. *J. Luminesc.* **1996**, 68, 35.